

# INVESTIGATION OF GRANULAR NATURAL STONE MATERIALS AS PHOTOTHERMAL ABSORBERS FOR SUSTAINABLE AND ENVIRONMENTALLY FRIENDLY ENERGY HARVESTING

Alfan Sarifudin<sup>1\*</sup>, Indri Yaningsih<sup>1\*</sup>, Budi Kristiawan<sup>1</sup>, Aditya Wibawa<sup>2</sup>, Takahiko Miyazaki<sup>3</sup>, Kyaw Thu<sup>3</sup>, Arridina Susan Silitonga<sup>4,5</sup>, Hwai Chyuan Ong<sup>6,7</sup>

<sup>1</sup> Department of Mechanical Engineering, Universitas Sebelas Maret, Surakarta, Indonesia

<sup>2</sup> Research Center for Geological Resources, National Research and Innovation Agency, Bandung, Indonesia

<sup>3</sup> Interdisciplinary Graduate School of Engineering Sciences, Kyushu University, Fukuoka, Japan

<sup>4</sup> Centre for Technology in Water and Wastewater, University of Technology Sydney, Sydney, Australia

<sup>5</sup> Department of Mechanical Engineering, Politeknik Negeri Medan, Medan, Indonesia

<sup>6</sup> Department of Engineering, School of Engineering and Technology, Sunway University, Selangor, Malaysia

<sup>7</sup> School of Civil and Environmental Engineering, University of Technology Sydney, Sydney, Australia

\* alfan.sarifudin@student.uns.ac.id; indriyaningsih@staff.uns.ac.id

The development of cost-effective and environmentally friendly solar thermal technologies that deliver high performance poses several challenges, where the collector and absorber components play a pivotal role. This research addresses these issues by investigating enhanced temperature generation using a 30 cm × 30 cm Fresnel lens collector under solar illumination from a xenon lamp. Natural stone materials (andesite, coal, and pumice), characterized by granular structures with an average diameter of 1.68–2.00 mm, were selected because of their abundance and eco-friendliness. This research is focused on evaluating the effect of Fresnel lens on temperature generation performance. Two types of temperature generation tests were carried out: wet tests (where the natural stone materials were immersed in distilled water) and dry tests (where the natural stone materials were used in dry conditions). The morphologies of the natural stone materials were examined using an optical microscope and scanning electron microscope. Furthermore, the optical properties of the natural stone materials were analyzed using an ultraviolet–visible (UV–VIS) spectrophotometer. The findings revealed that there were significant improvements in the photothermal absorber performance with the use of a Fresnel lens in dry tests, where the highest temperature was achieved for coal (103.25 °C), followed by andesite (89.00 °C) and pumice (73.00 °C). The impurities varied between the materials, where the impurities were most dominant for pumice while coal was more uniform. Further examination using scanning electron microscope showed that all materials had light-trapping structures in the form of rough surfaces, pores, and crack gaps. Andesite was dominated by rough surfaces, while coal and pumice were dominated by crack gaps and pores, respectively. However, based on the UV–VIS spectrophotometric results, there were no correlations between the optical properties (absorbance, reflectance, and transmittance) and temperature achieved by the photothermal absorber materials. This research demonstrates the potential of using natural stone materials as photothermal absorbers in combination with a Fresnel lens collector for low-to-medium temperature solar thermal applications.

**Keywords:** andesite, coal, fresnel lens, pumice, solar collector, solar energy

## 1 INTRODUCTION

Temperature is one of the key parameters used to assess the performance of photothermal absorbers when converting radiant energy into heat energy. Absorber and collector, which are the primary components of solar thermal equipment, are essential for temperature generation. Bie et al. [1] classified solar thermal applications based on temperature: low (<80 °C), medium (80–250 °C), and high (>250 °C). Apart from being designed with a suitable temperature, solar thermal technologies must be incorporated with economic benefits to make them more attractive for commercial purposes. Moreover, solar thermal technologies must be used in conjunction with natural or renewable materials to generate sustainable energy.

To address this problem, natural stone materials are proposed for use as photothermal absorbers because they do not pollute the environment. In addition, abundant natural stone materials are considered more economical than materials with engineered and purified chemical structures. Natural stone materials generally have granular structures with various sizes.

Granular structures act as light traps, increasing photothermal performance. Naturally arranged granular materials form rough and hollow surface structures such as pores. Olivernesaraj and Sethuramalingam [2] proved that a rough surface structure could increase the light-trapping effect. Nguyen et al. [3] and Zhang et al. [4] demonstrated that porous structures increased the light-trapping effect. Ultimately, the light-trapping effect increased the absorbance and decreased the reflectivity of absorber materials [5].

Several natural stone materials with granular structures have been tested in previous studies using direct sunlight, achieving low to medium temperatures. The most common collector used in previous studies is the flat plate collector or similar structure with a maximum solar concentration ratio of 1. Mohamed et al. [6] used basalt stones in a flat

plate collector and obtained a maximum temperature of 63.7 °C. Bilal et al. [7] used pumice stones and achieved a maximum temperature of ~74 °C. Arunkumar et al. [8] used pebbles and obtained a maximum temperature of 57.4 °C. López-Sosa et al. [9] used gravel and limestone, attaining a maximum temperature of 60 °C. Elmaadawy et al. [10] used gravel and produced a maximum temperature of 71 °C. Naik and Shekhar [11] used black-coated pebbles and attained a maximum temperature of ~63 °C. Attia et al. [12] used a hemispherical collector with black gravel, producing a maximum temperature 69 °C. From the aforementioned studies, the achieved temperatures can only be classified as low temperatures because the collectors used have a maximum solar concentration ratio of only 1. By contrast, Elashmawy [13] used a collector with a higher solar concentration ratio and a parabolic trough tracking reflector to test the performance of gravel, obtaining a maximum temperature of 103 °C. Therefore, the use of collectors with high solar concentration ratios exhibits the potential to increase the temperature generation of photothermal absorbers.

One of the collectors with a solar concentration ratio equivalent to that of a parabolic trough collector is the Fresnel lens collector [14], [15]. Previous studies have succeeded in creating Fresnel focal point innovations to boost the concentration of light. Pandi et al. [16] combined an evacuated tube receiver with a Fresnel lens and *CuO* nanoparticle fluid for a photothermal absorber, achieving a maximum temperature of 89 °C. According to the temperature classification established by Bie et al. [1], Fresnel lens collectors can be used for medium temperature applications. Furthermore, Fresnel lens collectors produce higher temperatures than flat plate collectors due to their higher light concentration and lower heat loss [17]. A study conducted by Asrori and Susilo [18] using a Fresnel lens to heat 2 liters of water found a temperature of around 70 °C, but they did not report the type of absorber used. Furthermore, the Fresnel lens application also has the potential to be used for steam generation [19] and solar cookers [20]. Moreover, Rashid et al. [21] reported in their review study that Fresnel lenses have broad applications such as photovoltaics, solar stills, solar thermal collectors, solar sterilization, solar cookers, and solar-pumped lasers.

This research aims to determine the effect of using a Fresnel lens collector on the temperatures achieved by andesite, coal, and pumice granular structural materials. These natural stone materials were selected based on their wide availability and affordable prices. Moreover, the natural stone materials were obtained without chemical reactions, exhibiting properties that are not detrimental to the environment. The following variables were considered for the experiments: (1) use of Fresnel lens, (2) without the use of Fresnel lens, (3) wet conditions (where the natural stone materials were immersed in distilled water), and (4) dry conditions (where the natural stone materials were used in dry conditions). The morphologies of the natural stone materials were examined by optical microscopy while their optical properties were examined by ultraviolet–visible (UV–VIS) spectrophotometry. Further analysis was carried out to examine the morphologies of the natural stone materials in more detail by scanning electron microscopy (SEM) and their elemental compositions by energy-dispersive X-ray (EDX) spectroscopy. The potential of each natural stone material was assessed under different conditions.

## 2 MATERIALS AND METHODS

Andesite, coal, and pumice from nature in the form of chunks that were dirty and nonuniform in size were used in this research. Therefore, the materials needed to be preprocessed to obtain uniform-sized materials and remove impurities such as soil, plastic, tree branches, etc., as presented in Figure 1.

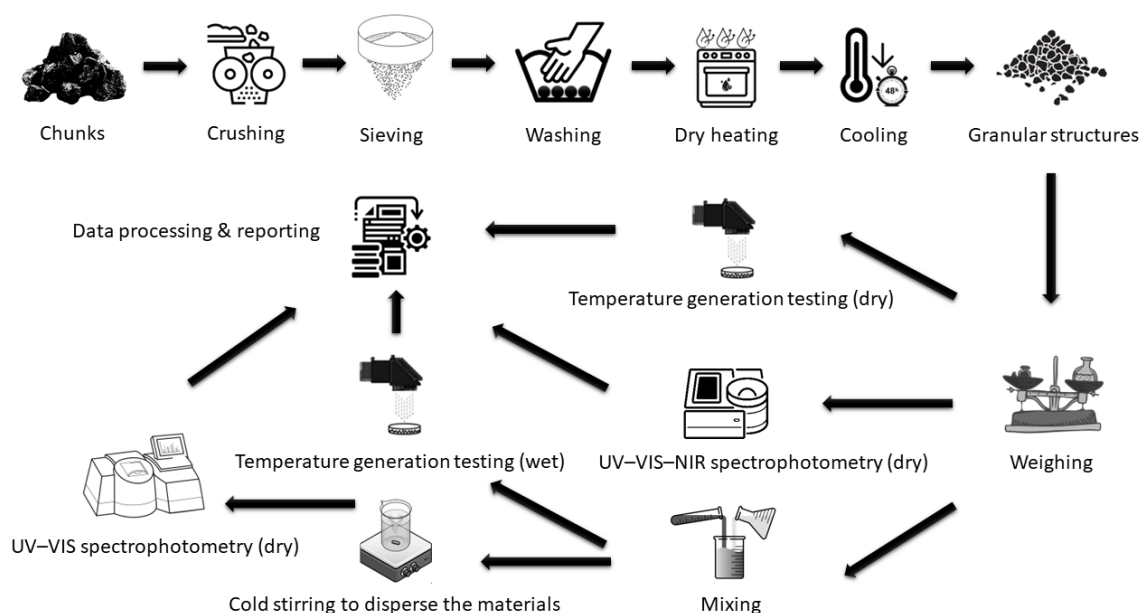


Fig. 1. Preprocessing of the materials and experiments

The natural stone materials used in this research are presented in Figure 2.

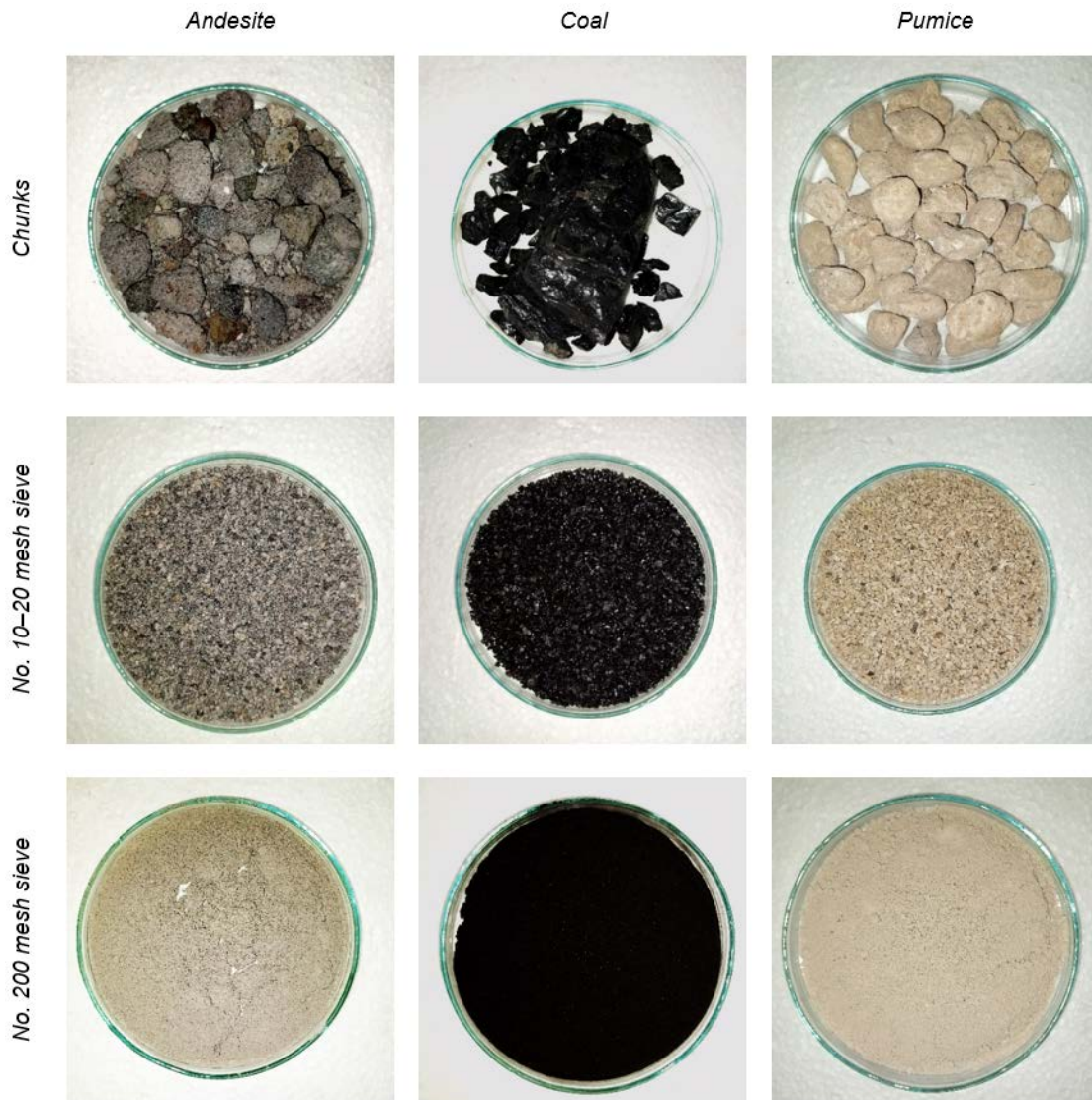


Fig. 2. Natural stone materials used in this research

## 2.1 Temperature Generation Tests

Specimens were prepared from chunks of natural rocks, which were then crushed. Following this, the crushed materials were sieved by passing the natural stone materials through a No. 10 mesh sieve. The materials were then retained using a No. 20 mesh sieve. Next, the sieved materials were washed using water to obtain clean materials. Apart from removing dirt on the materials, washing removes refined grains covering the pores of the materials. The cleaned materials were then dried in an oven at 150 °C for 3 h. After drying, the materials were left to cool to room temperature in an open space for 48 h. The materials used for the temperature generation tests are presented in the second row of Table 1.

The dried materials were then tested to determine the temperature that can be achieved by these materials using a Fresnel lens collector under  $1000 \text{ W/m}^2$  (one solar illumination) from a xenon lamp. The temperature generation tests were also carried out without a Fresnel lens (direct radiation). The power of the xenon lamp was 100 W at a DC voltage of 12 V. The temperature generation tests were conducted at a controlled room temperature of  $25 \pm 1 \text{ }^\circ\text{C}$  and relative humidity of 51.6–82.2% for 1200 s. The thermometer used to measure the room temperature has an accuracy of 0.25 °C with a maximum error of  $\pm 2 \text{ }^\circ\text{C}$ . The hygrometer used to measure the relative humidity has an accuracy of 0.1% with a maximum error of  $\pm 3\%$ . Two types of tests were carried out in this research: (1) dry tests and (2) wet tests. For the dry tests, 20 g of granular materials were used. For the wet tests, 20 g of granular materials were immersed in 20 g of distilled water.

This research is a laboratory-scale experiment to test the photothermal conversion properties of materials under controlled conditions with light intensity that is always the same for each test so that each variable can be compared. Direct solar radiation for partial testing will result in each variable being unreliable for comparison because sunlight constantly changes in intensity with changes in time and weather. To overcome this problem, previous researchers tested their specimens under sunlight simultaneously. Considering this research examines up to 6 specimens then 6 Fresnel lens collectors must be used simultaneously for direct sunlight testing. Therefore, testing with direct solar radiation is impractical and too expensive for many variables. Thus, the test method using xenon lamp simulation

provides the advantage of flexible time, is not affected by weather, reliable data for partial tests, and is more cost-effective for tests with many variables. Furthermore, xenon lamps and halogen lamps are sources of artificial light radiation closest to sunlight conditions [22]. Therefore, previous research has used xenon lamp light as a simulated sunlight source for photothermal absorbers. Several previous studies used xenon lamps as an artificial sun to test photothermal properties, including Bao et al. [23] to test photothermal conversion, Zhang et al. [24] to test photothermal storage, Liu et al. [25] to test photothermal@electrothermal, and so on.

## 2.2 Morphologies

The morphologies of the natural stone materials in dry conditions were examined using an optical microscope with a magnification of 100–200 times. The materials tested were those sieved using a No. 200 mesh sieve (Table 1). The morphologies were examined to analyze the presence of light-trapping structures in the material grains and the gaps between the grains. The morphologies of the materials were further examined by scanning electron microscopy (SEM) [26]. Furthermore, the elemental compositions of the materials were examined by energy dispersive X-ray (EDX) spectroscopy or energy-dispersive X-ray spectrometry (EDS) [27].

## 2.3 Optical Properties

The optical properties of the natural stone materials were examined by UV–VIS spectrophotometry in dry and wet conditions. In dry UV–VIS spectrophotometry, the materials sieved using No. 10 and 20 mesh sieves were tested at an ultraviolet A–visible–infrared wavelength range of 315–1100 nm.

In wet UV–VIS spectrophotometry, the materials sieved using the No. 200 mesh sieve were used. The weight of each material for each liquid sample was 0.1 g. The materials were weighed using an analytical balance with an accuracy of 0.0001 g. The materials were first mixed with 20 mL of distilled water to form liquid samples. Following this, the liquid samples were stirred using a magnetic stirrer for 30 min at a room temperature of  $30 \pm 3$  °C. Next, the liquid samples were tested using a UV–VIS spectrophotometer within a wavelength range of 200–800 nm. The optical properties determined were the absorbance, reflectance, transmittance, and energy.

To ensure the liquid samples were still in good condition, the samples must be tested immediately, no more than 10 min after dispersion of the materials. The liquid samples that had expired were precipitated, resulting in clear solutions.

## 3 RESULTS AND DISCUSSION

### 3.1 Temperature Generation Tests

#### 3.1.1 Wet tests

The purpose of the wet temperature generation tests was to assess the ability of the natural stone materials to convert radiant energy into heat when the materials were immersed in distilled water. The submerged test conditions represent photothermal applications such as heat harvesting and vapor generation harvesting. Mohamed et al. [6] used the submerged solar absorber design for solar desalination using a basalt stone absorber. The results of the wet temperature generation in direct radiation tests obtained in this research are presented in Figure 3 (a).

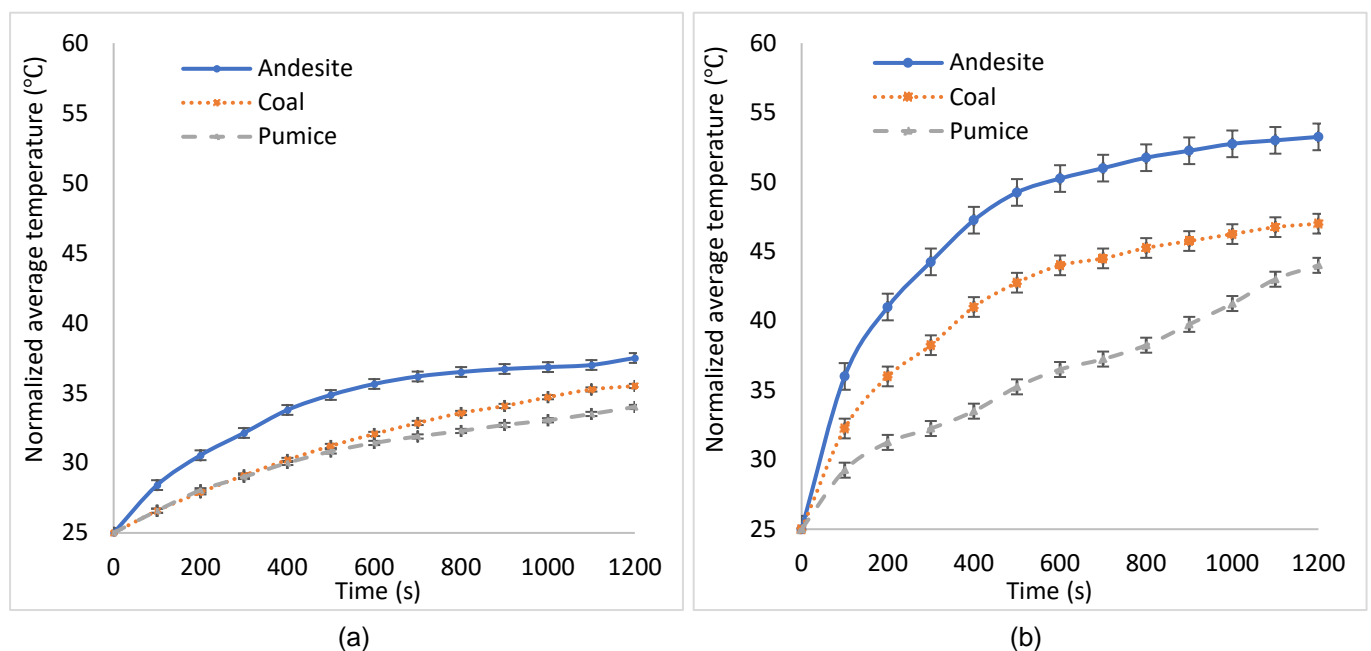


Fig. 3. Wet temperature generation test results where the natural stone materials were immersed in distilled water: (a) direct radiation and (b) using a Fresnel lens

Based on the direct radiation test results, the natural stone that produced the highest temperature was andesite (37.50 °C). Meanwhile, coal and pumice produced a temperature of 35.50 and 34.00 °C, respectively. These temperatures are suitable for vapor generation in solar desalination or solar still applications. Several studies using different materials and structures reported the application of vapor generation at temperatures ranging from 20 °C to 33 °C tested at 1 kW/m<sup>2</sup> of irradiation. Mu et al. [28] increased the temperature from 20 °C to 30 °C using kapok fiber aerogels. Jia et al. [29], using attapulgite/poly(acrylamide) composite material, obtained a temperature of 33 °C. Lim et al. [30] tested a 3D hydrogel-based solar absorber at an ambient temperature of 24–25 °C and obtained a temperature generation of 26 and 30 °C for polyacrylate (PA) hydrogel and polypyrrole/alginate/poly(n-isopropylacrylamide) hydrogel, respectively.

Meanwhile, the test results obtained using a Fresnel lens (Figure 3 (b)) showed that the temperature achieved was higher than those obtained without the use of Fresnel lens for all natural stone materials. Andesite achieved the highest temperature, with a value of 53.25 °C. In comparison, coal and pumice materials produced a temperature of 47.00 and 44.00 °C, respectively. With a significant increase in temperature, the heat flux will increase, resulting in better vapor generation [31]. Rajiv Krishnan [32] found that solar stills should be designed to focus the incident solar radiation on the absorber, which will increase the efficiency of the solar stills. Apart from using a Fresnel lens, the incident solar radiation can also be focused by directing light to the absorber using mirrors, as done by Alaskaree [33].

Moreover, the temperature achieved can also be applied to warm water in households. The temperature of warm water typically falls within a range of 36–45 °C and generally exceeds 40 °C [34]. The higher temperatures achieved for andesite and coal can be lowered by mixing the materials with more water. Therefore, there is no need to waste the heat energy obtained. However, the temperatures achieved for all absorbers do not meet the requirements for hot water in distributed housing districts since the temperatures achieved were less than 60 °C [35].

### 3.1.2 Dry tests

Dry temperature generation tests were performed to assess the ability of the materials to convert solar radiation energy into heat where the materials were used in dry conditions, which is representative of heating applications. To heat liquids, a heat exchanger is needed to separate direct contact between the liquid and absorber but still transfers heat from the absorber to the liquid. The design concept of rocks as a photothermal absorber in dry conditions for water heating has been used by Wirawan et al. [36]. They used aa flat plate collector with a copper tube heat exchanger. Therefore, heat exchange takes place by conduction. To heat air, the system does not require a heat exchanger because the air can directly flow to the absorber to establish contact between the air and absorber. The use of granular rocks as photothermal absorber for air heating without additional heat exchangers has been applied by Kumar et al. [37]. Furthermore, the rocks used in their research also function as heat storage. Therefore, heat exchange occurs by conduction and convection.

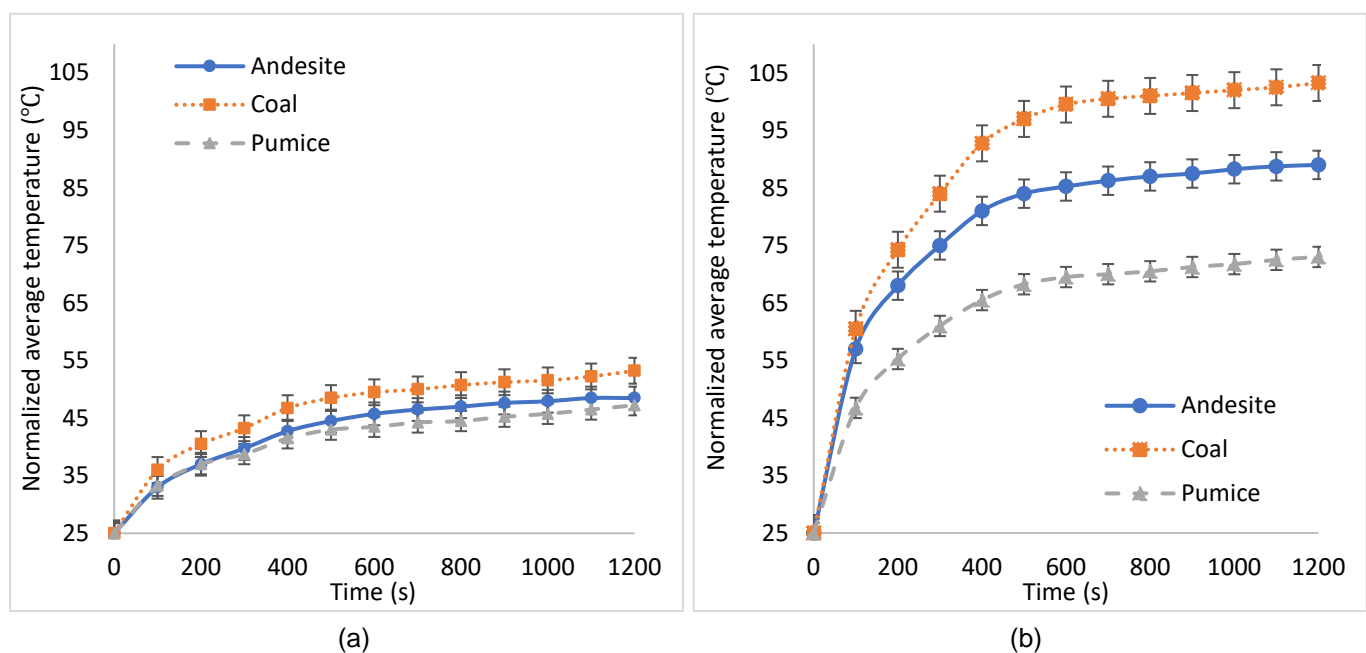


Fig. 4. Dry temperature generation test results where the natural stone materials were used in dry conditions: (a) direct radiation and (b) using a Fresnel lens

The direct radiation test results (Figure 4 (a)) showed that the material with the most optimal performance was coal, where the temperature achieved was 53.25 °C. The temperatures achieved for andesite and pumice were 48.5 and 47.25 °C, respectively. It is worth noting that that the most optimal materials for wet and dry tests were different. In the wet tests, the most optimal material was andesite, while in the dry test, it was coal. Coal and pumice are more porous, causing them to absorb more water in wet tests. Therefore, there is a higher heat exchange from the material

to the fluid because the pores expands contact of the heat transfer surface [38]. This reduces the local heating of the area in the porous material when the material is immersed in water because gaps of cracks and holes of porosity will absorb more water. Therefore, in the wet tests, the temperature achieved for coal was lower than that for andesite, even though the result was opposite in the dry tests. To determine the presence of porous structures, SEM testing is carried out. For all materials, the temperatures produced in the wet tests were lower than those in the dry tests. This occurs because in wet tests, the absorber has an immersion cooling effect where water can absorb heat better than air [39].

The photothermal absorber materials tested in this research (andesite, coal, and pumice) in dry conditions without using a Fresnel lens have the potential for water heating applications in households because they work above the required range. Therefore, water fractions should be added to obtain a temperature that suits a particular application. All of these materials also have the potential for drying certain agricultural products such as pistachios ( $50 \pm 10$  °C) [40] and paddy (45–55 °C) [41]. Andesite and pumice photothermal absorbers are suitable for drying coffee with an optimal drying temperature of 40–50 °C [42], [43]. Coal without Fresnel lens is suitable to dry fruits (50–70 °C) and preheat raw materials (50–80 °C) [44], [45]. Furthermore, coal without using a Fresnel lens is ideal for sterilization of *E. coli* because the thermal deformation temperature of these bacteria is 51 °C [46]. Isah et al. [47] succeeded in producing distilled water without *E. coli* using granular charcoal in solar desalination of seawater containing 54.8/100 mL *E. coli*. It is better to use the recommended temperature to dry agricultural products. The drying rate is ineffective and inefficient if the temperature is too low. However, the agricultural products will be damaged if the temperature is too high. Moreover, solar dryers should be designed based on practical experience, local climate, and economic conditions [48].

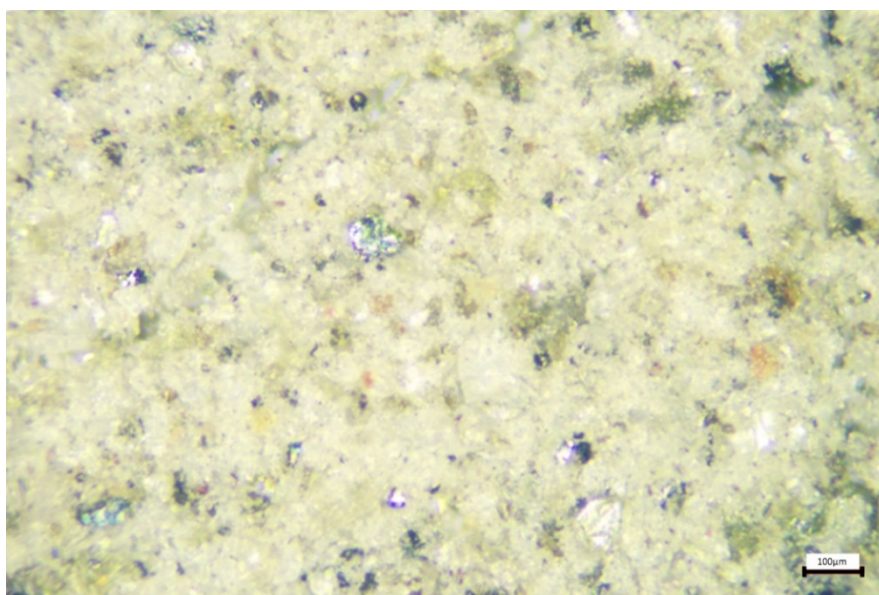
The results of the dry tests also indicate that the natural stone materials are unsuitable for use as building facades in tropical regions or areas with intense exposure to sunlight and heat. The resultant temperatures of the materials (47.25–53.25 °C) can cause discomfort for building occupants. Liu et al. [49] found that the physiological equivalent temperature for the normal category in the tropics was 26.3–31.7 °C. The solution offered can be in the form of coating using materials which will result in a lower temperature. Building facades can also be wetted, as proven by the wet tests, where the temperatures produced by the natural stone materials were lower.

The results of the temperature generation test in dry conditions with focused light using a Fresnel lens are presented in Figure 4 (b). A drastic increase in temperature was obtained in the dry tests with the use of a Fresnel lens compared with that without a Fresnel lens, where the most optimal material was coal (103.25 °C). The temperatures generated by andesite and pumice were 89.00 and 73.00 °C, respectively. Based on the classification of Bie et al. [1], coal and andesite photothermal absorbers can be used for medium temperature applications whereas pumice can be used for low temperature applications. All of the granular materials tested in this research with the use of a Fresnel lens fulfill the European Union (EU) standard of at least 60 °C [35] for distributed water heating. Moreover, these materials are suitable for industrial processes for pharmaceuticals (70–180 °C) [1].

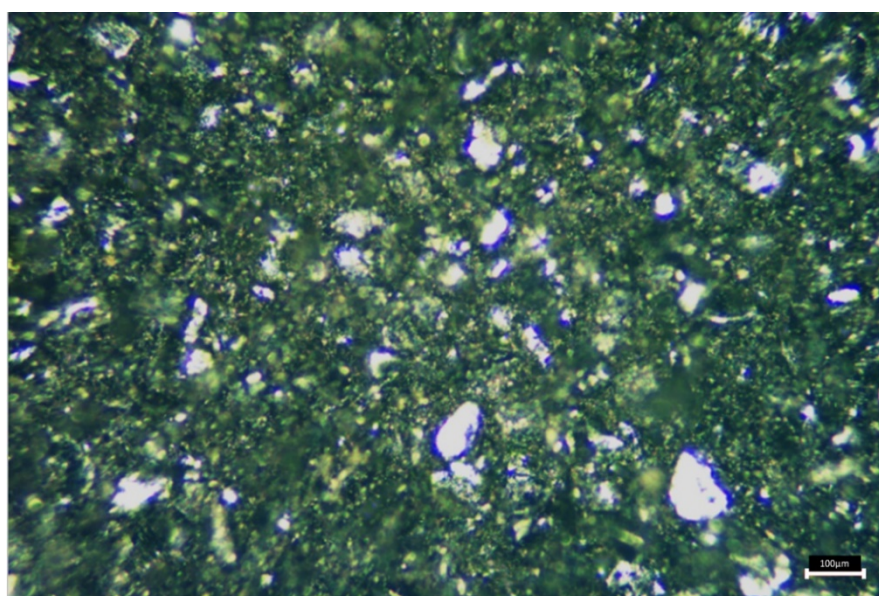
To determine the significance of the variables tested in a multivariate manner, nonparametric multivariate analysis of variance (MANOVA) was used since this method does not require normal and homogeneous data [50]. The temperature data used was transient from 1 s to 1200 s. The *p*-values of the results of the one-way and two-way MANOVA were 0.000, indicating that the use of a Fresnel lens and natural stone materials significantly affect the temperature generated by the photothermal absorber in wet and dry tests.

### 3.2 Morphologies

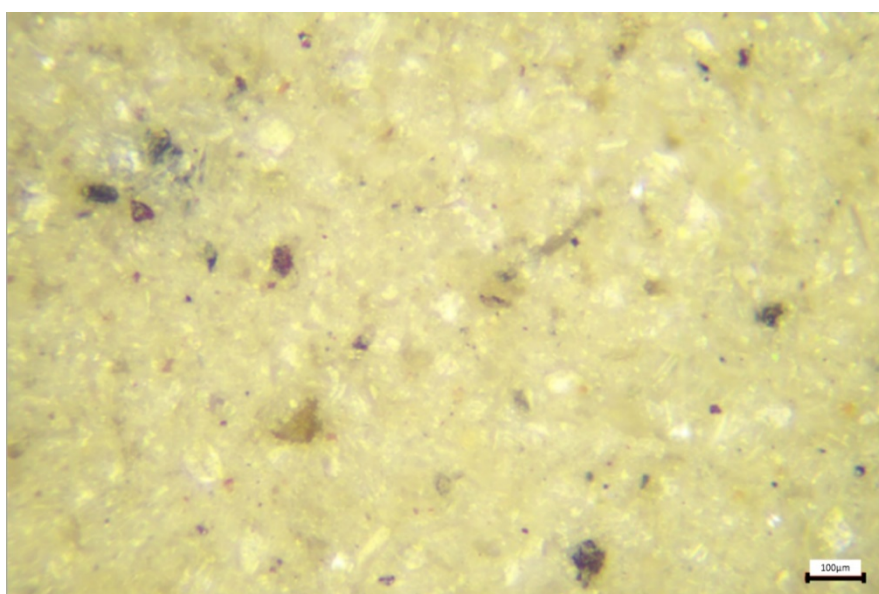
Figure 5 shows the images obtained from an optical microscope with a magnification of 100–200 times. It can be observed that all of the natural stone materials showed no material porosity. Andesite (Figure 5 (a)) and pumice (Figure 5 (c)) were highly nonuniform, as indicated by the patches of darker contrasting colors. Coal (Figure 5 (b)) was also nonuniform though the nonuniformity was not as marked as those for andesite and pumice, as indicated by the yellow spots, which were suspected to be soil contaminants. This nonuniformity is indeed expected because the natural stone materials are unrefined materials. Pores were not observed for all of the materials based on the images obtained using the optical microscope. However, the surfaces of all the materials appeared rough. Pores are one of the light-trapping structures that can improve photothermal performance by trapping light in narrow slits. A porous structure will also improve photothermal performance for steam and vapor generation applications. Ma et al. [51] developed a light-trapping structure using porous carbon for solar steam generation. Li et al. [52] developed porous hybrid nanohydrogels for vapor generation. Meanwhile, a rough surface is also a light-trapping structure which increases the surface area of the material that receives light. The phenomenon of surface roughness as a light-trapping structure has been proven by Gao et al. [53] using wrinkled nanocone surface enhanced Raman spectroscopy (SERS) substrate materials.



(a)



(b)

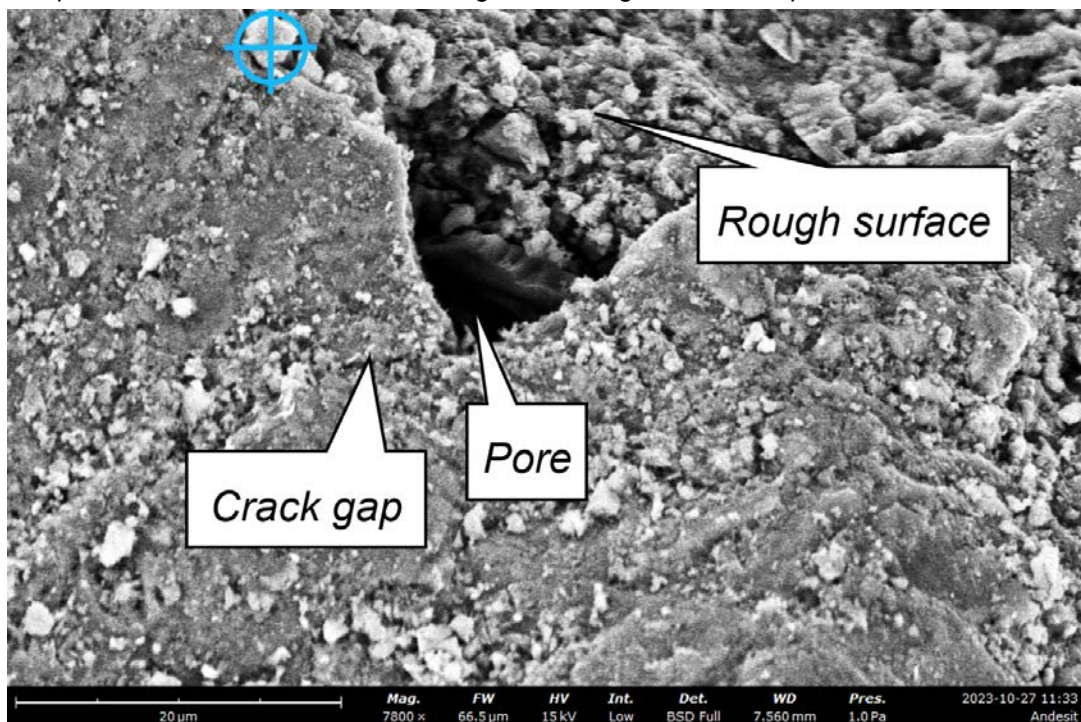


(c)

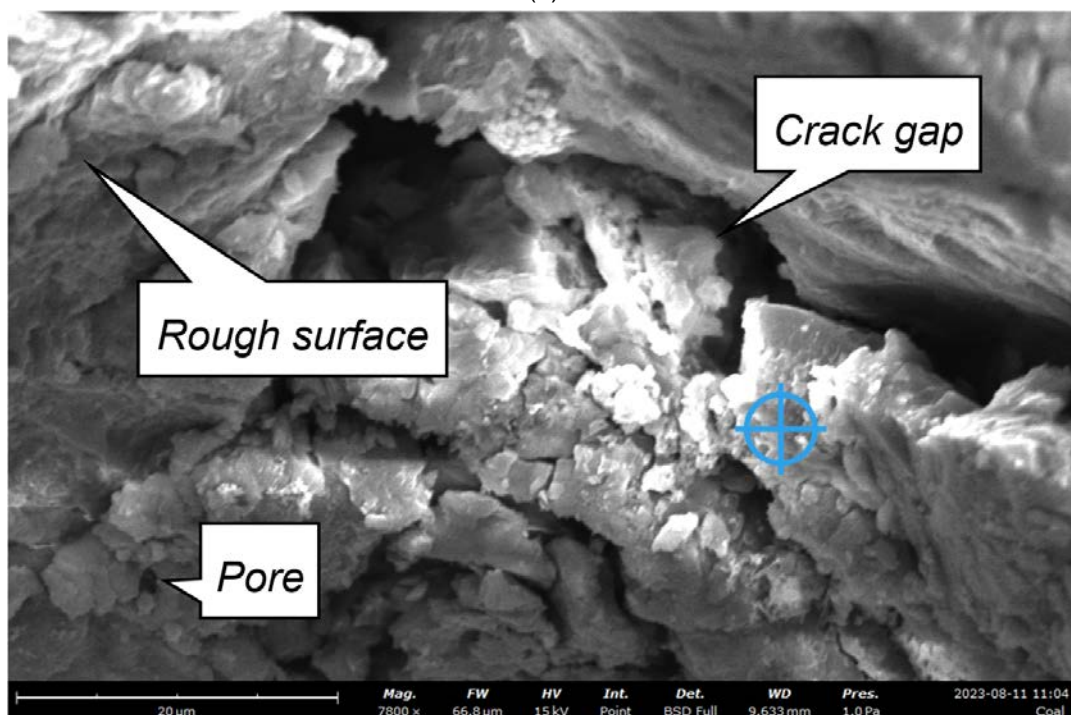
Fig. 5. Morphologies of (a) andesite, (b) coal, and (c) pumice obtained using an optical microscope

The absence of pores in the natural stone materials observed using an optical microscope may be due to the following reasons: (1) insufficient optical magnification or (2) the materials were indeed not porous. Therefore, the materials were further examined using a scanning electron microscope. In addition, EDX spectrometer was used to determine the elemental compositions of the materials.

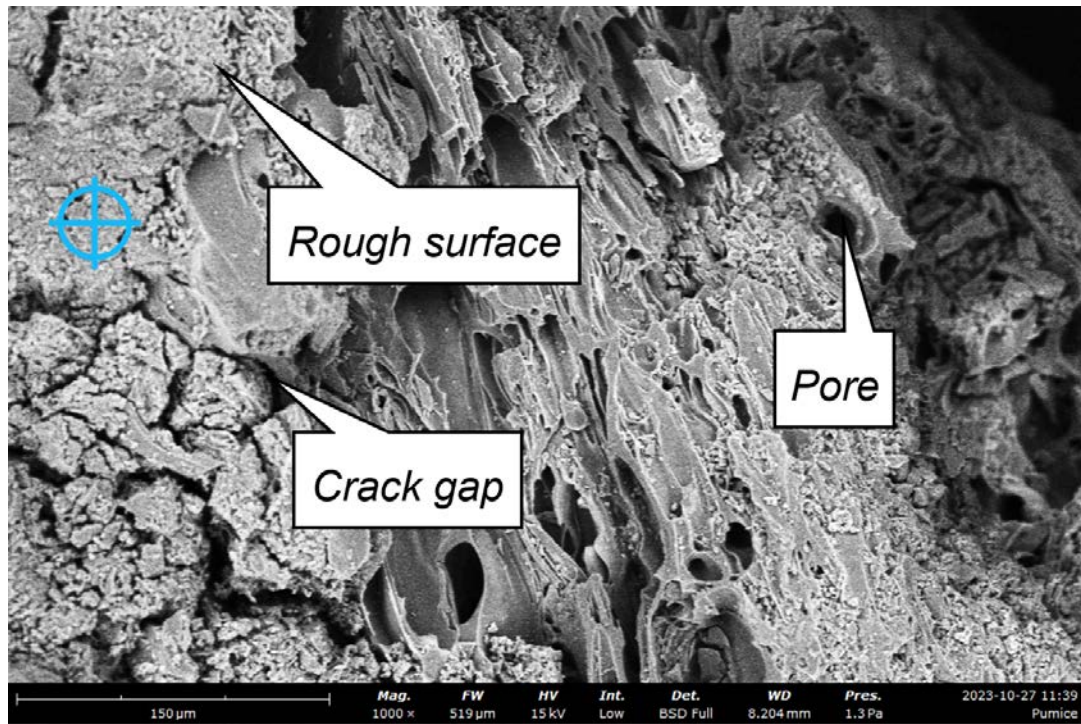
Figure 6 (a), (b), and (c) show that each material had light-trapping structures in the form of crack gaps, pores, and rough surfaces. Several studies have confirmed that holes [54], rough surfaces [55], and pores [56] can improve the light absorbance of photothermal absorbers. Figure 6 also shows that there were crack gaps in the materials, which can be classified as light-trapping structures. For andesite (Figure 6 (a)), the light-trapping structures were dominated by rough surfaces whereas crack gaps and pores were not dominant. Hence, when andesite is submerged in water, it does not absorb much water, which in turn, does not significantly affect the immersion cooling effect. This explains why in the wet tests, the temperature achieved for andesite was higher than that of coal, even though in the dry tests, the temperature of andesite was lower. As for coal (Figure 6 (b)), the light-trapping structures were dominated by crack gaps whereas for pumice (Figure 6 (c)), the light-trapping structures were dominated by pores. Structures with crack gaps and pores tend to absorb water, resulting in a lower generated temperature in the wet tests.



(a)



(b)



(c)

Fig. 6. SEM images: (a) andesite, (b) coal, and (c) pumice

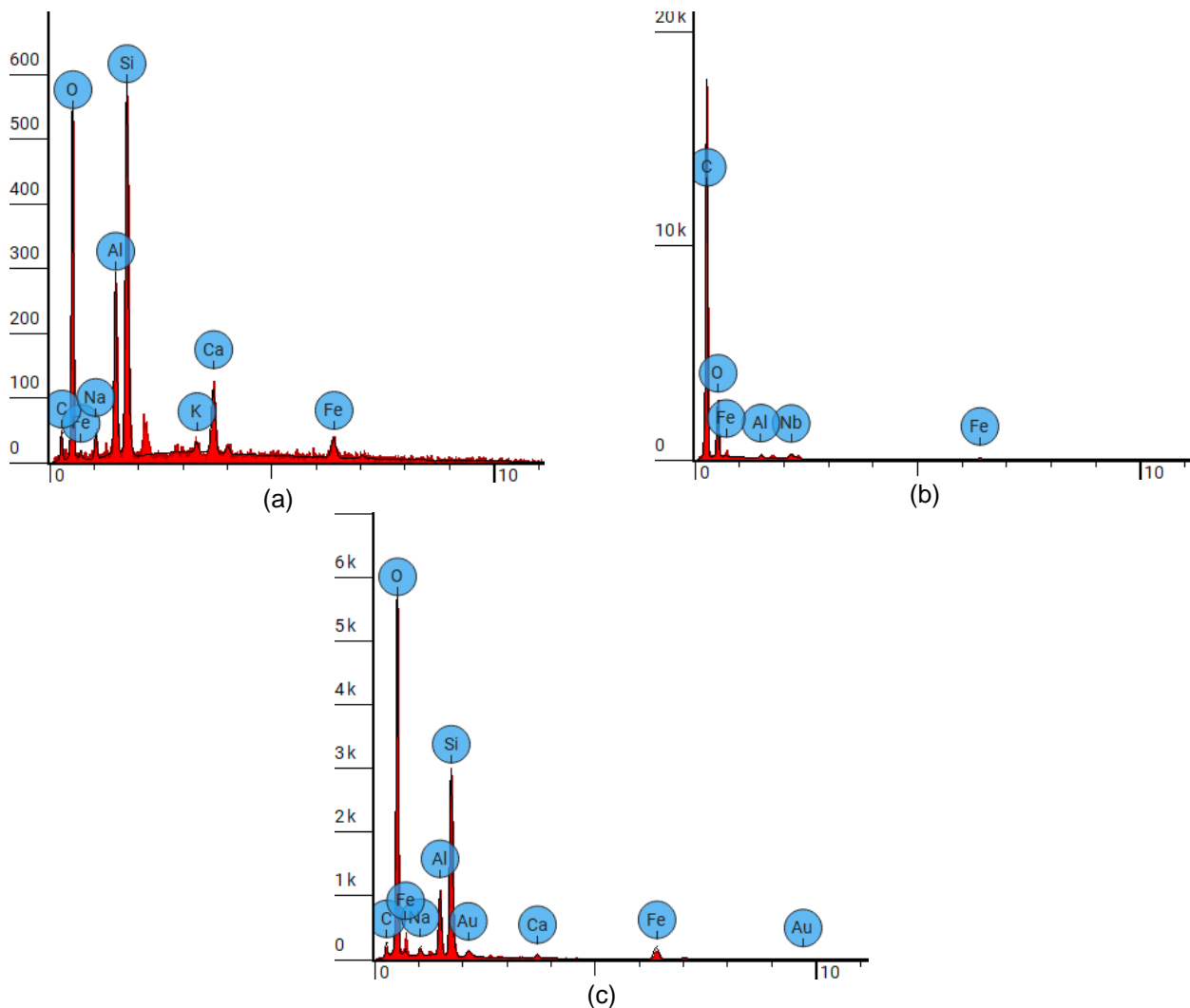


Fig. 7. EDX spectra: (a) andesite, (b) coal and (c) pumice

The EDX spectra for all materials investigated in this research are shown in Figure 7 (a), (b), and (c), and the elemental compositions of the materials are summarized in Table 1. Overall, the main element that constituted the natural stone materials was carbon. Therefore, the higher the carbon content, the better the generated temperature because carbon-based materials have high photothermal conversion efficiency based on the super-conjugate effect [57].

Table 1. Elemental compositions of andesite, coal, and pumice

Materials	Element number	Element symbol	Element name	Atomic concentration (%)	Weight concentration (%)
Andesite	6	C	Carbon	14.835	8.509
	8	O	Oxygen	50.568	38.639
	11	Na	Sodium	1.823	2.002
	13	Al	Aluminum	9.326	12.012
	14	Si	Silicon	14.626	19.620
	19	K	Potassium	0.911	1.702
	20	Ca	Calcium	4.759	9.109
Coal	26	Fe	Iron	3.153	8.408
	6	C	Carbon	78.073	70.110
	8	O	Oxygen	20.792	24.875
	13	Al	Aluminum	0.298	0.602
	26	Fe	Iron	0.504	2.106
Pumice	41	Nb	Niobium	0.332	2.307
	6	C	Carbon	12.413	7.493
	8	O	Oxygen	62.864	50.549
	11	Na	Sodium	1.124	1.299
	13	Al	Aluminum	6.191	8.392
	14	Si	Silicon	13.021	18.382
	20	Ca	Calcium	0.546	1.099
	26	Fe	Iron	3.559	9.990
79	Au	Gold	0.282	2.797	

### 3.3 Optical properties

The absorbance of a photothermal absorber  $\alpha_s$  is the ratio of the fraction between the absorbed radiation and incoming solar radiation, as given by equation 1 [58].

$$\alpha_s(\theta, \lambda) = \frac{\int_{\lambda_{min}}^{\lambda_{max}} [1 - (R + T)(\theta, \lambda)] [I_s(\lambda)] d\lambda}{\int_{\lambda_{min}}^{\lambda_{max}} [I_s(\lambda)] d\lambda} \quad (1)$$

where  $\theta$  is the light incidence angle,  $\lambda$  is the wavelength, R is the reflectance, T is the transmittance, and  $I_s$  is the direct normal solar irradiance.

The relationship between light absorbance and transmittance (%T) in the dry tests is given by a logarithmic function (equation 2). The absorbance can also be determined from the logarithmic function of the incident light ( $I_o$ ) and transmitted light ( $I$ ) (equation 3). The absorbance spectra of andesite, coal, and pumice with a microgranular structure in dry conditions are presented in Figure 8 (a).

$$\alpha_s = \log_{10} \left( \frac{1}{\%T} \right) \quad (2)$$

$$\alpha_s = \log_{10} \left( \frac{I_o}{I} \right) \quad (3)$$

The transmittance is calculated from the relationship of the transmitted light ( $I$ ) to the incident light ( $I_o$ ) (equation 4). The transmittance spectra of andesite, coal, and pumice with a microgranular structure in dry conditions are shown in Figure 8 (b).

$$\%T = \frac{I}{I_o} \quad (4)$$

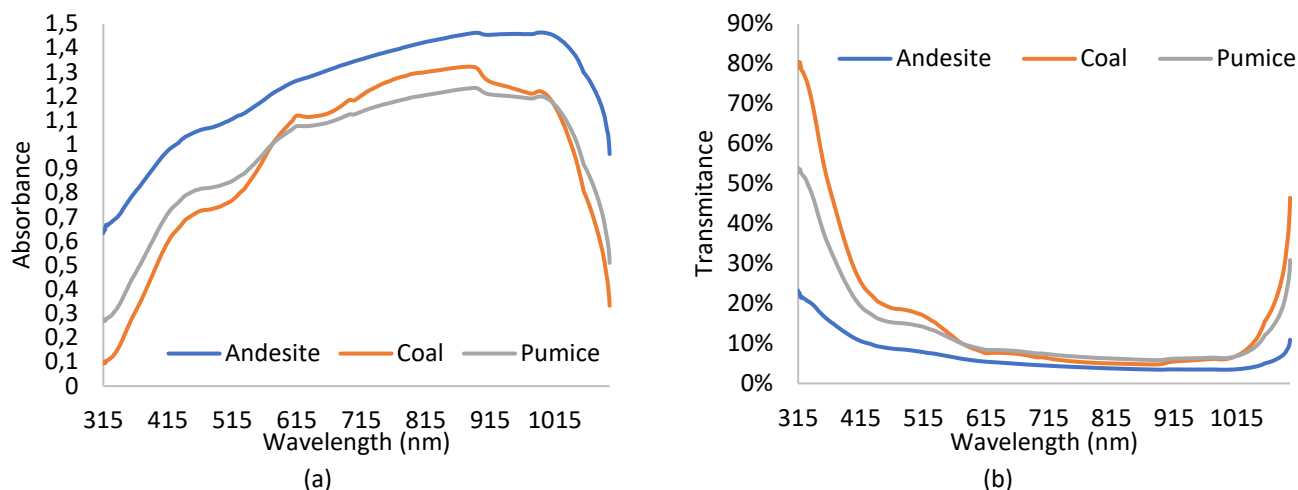


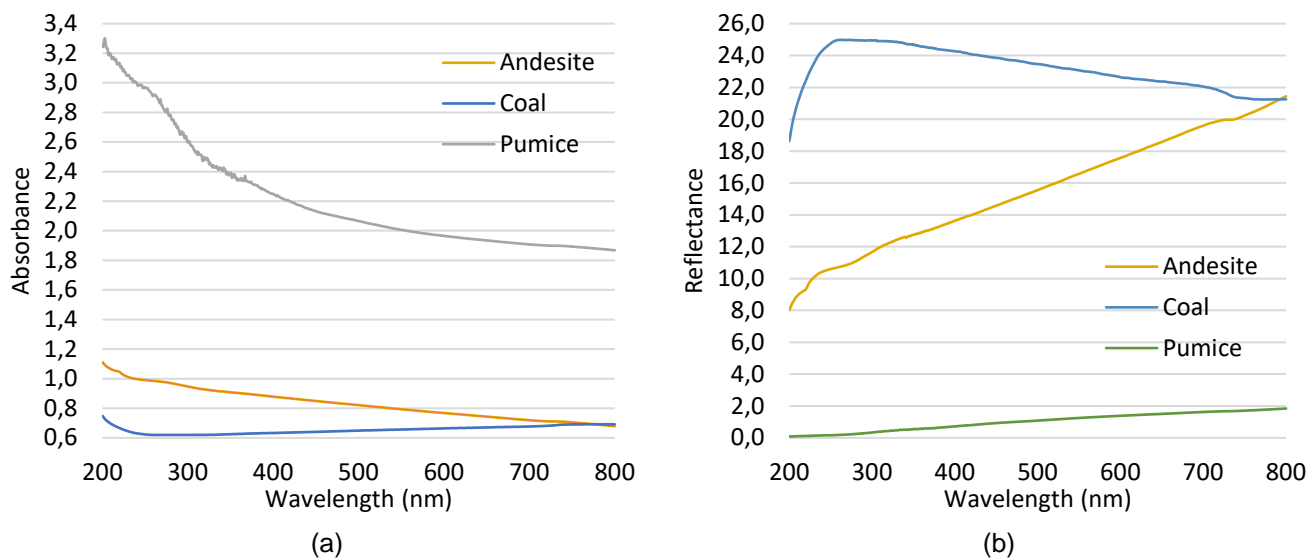
Fig. 8. Optical properties of andesite, coal, and pumice in dry conditions: (a) absorbance and (b) transmittance

The absorbance of the natural stone materials used as photothermal absorbers in dry conditions are presented in Figure 8 (a). The material with the highest absorbance in the UVA–VIS–IR wavelength range was andesite. Meanwhile, the absorbance of coal was higher than that of pumice within a wavelength range of 578–1012 nm. The transmittance of the materials in dry conditions are presented in Figure 8(b) and the transmittance showed the opposite trend of the absorbance, forming U-shaped curves. The absorbance of the natural stone materials with a microgranular structure in wet conditions are presented in Figure 9 (a). The material with the highest UV–VIS absorbance in wet conditions was pumice, followed by coal, and least of all, andesite.

The results of the dry and wet spectrophotometry showed that there was no correlation between the absorbance and generated temperature of the natural stone materials. These results align with the experimental results of Amjad et al. [59], who tested various nanofluids and found that Si had a higher average absorbance than Fe and Cu, but the temperature generated by Si was lower. In addition, visible light tests showed that graphene oxide (GO) had higher absorbance than silver [60], [61], but the temperature generated by silver was higher [61]. However, other researchers using the same materials with different concentrations found that higher absorbance resulted in higher generated temperatures [62]–[65]. Therefore, absorbance influences the generated temperature; however, other material properties may have a greater influence on the generated temperature for different material types.

Pumice had the highest light absorbance compared with andesite and coal. Light is more dominantly absorbed at shorter wavelengths in the UV region. The reflectance (Figure 9 (b)) and transmittance (Figure 9 (c)) spectra showed similar trends though the values were different. The material with higher absorbance had lower transmittance and reflectance values. The relationship between absorbance, transmittance, and reflectance observed in this research align with the results of Abed et al. [66] using  $Co_3O_4 - Cr_2O_3$  nanocomposites.

The energy resulting from exposure to UV–VIS light was highest for coal, followed by andesite and pumice, as shown in Figure 9 (d). These results correspond with the dry temperature generation tests. The peak area of energy generation was in the UV region and the energy decreased at longer wavelengths. The right photothermal materials with high energy is the key to optimize the efficiency of converting photons to heat [67].



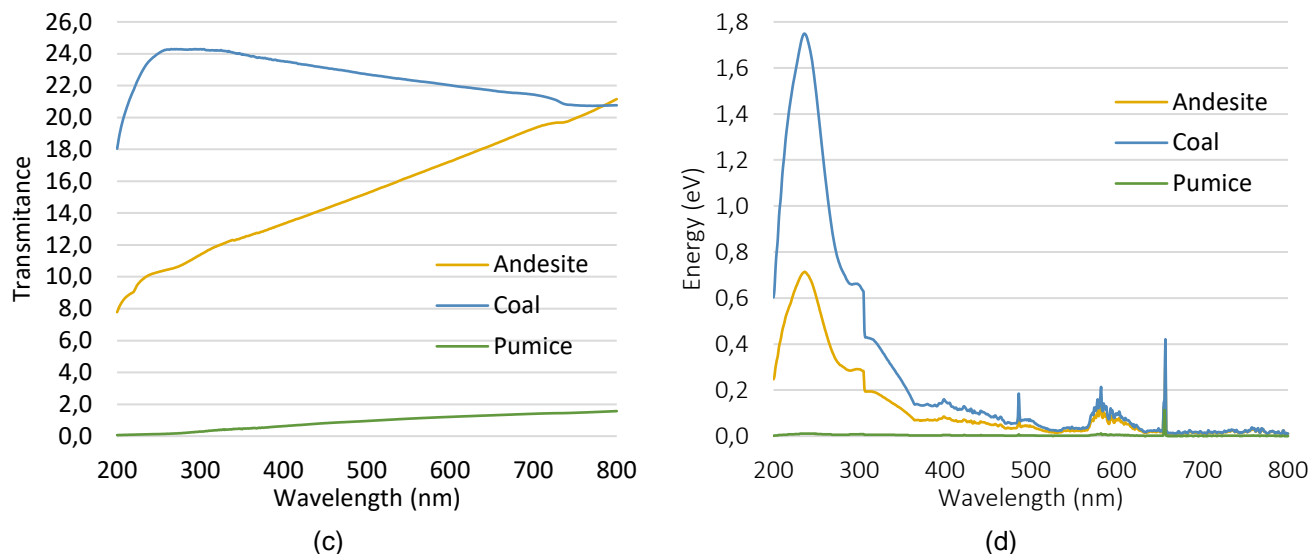


Fig. 9. Optical properties of andesite, coal, and pumice in wet conditions: (a) absorbance, (b) reflectance, (c) transmittance, and (d) energy

#### 4 CONCLUSIONS

Based on the results of experimental data and discussion, it was concluded that:

- The use of Fresnel lens significantly increased the generated temperature of andesite, coal, and pumice photothermal absorbers investigated in this research.
- The temperatures obtained were higher in dry temperature generation tests for all the natural stone materials compared with those in wet temperature generation tests.
- In wet tests, the most optimal material was andesite and in dry tests, the most optimal material was coal.
- The morphologies observed using an optical microscope indicated that rough surfaces were present in andesite, coal, and pumice.
- Further examination using a scanning electron microscope revealed that all the materials had light-trapping structures in the form of rough surfaces, pores, and crack gaps.
- Rough surfaces, crack gaps, and pores were dominant in andesite, coal, and pumice, respectively.
- Based on the UV–VIS spectrophotometric results, there was no correlation between the optical properties (absorbance, transmittance, and reflectance) and the generated temperature of the photothermal absorber.
- Energy was found to be correlated with the temperature generation.

#### 5 LIMITATIONS, IMPLICATIONS AND SUGGESTIONS

In this research, temperature generation tests were conducted under open system conditions, where the heat released to the environment was considerable. For further research, it is recommended that the temperature generation tests should be carried out using a closed or isolated system to minimize heat losses and achieve a higher temperature. Moreover, the use of solar collectors with different solar concentration ratios will result in different temperatures, which can be exploited for different applications. Based on the morphologies of the tested materials, the granular structure of the materials act as light-trapping structures, indicating that the materials have potential as photothermal absorbers. The materials used for wet spectrophotometry in this research were microparticles, which can quickly precipitate. Hence, in future research, it is recommended to use nanomaterials. Meanwhile, based on the optical properties of the tested materials, further research is needed to analyze the energy generated for the tested materials since energy is associated with the generated temperature unlike absorbance, reflectance, and transmittance. This photothermal absorber research results imply that natural materials (andesite, coal, and pumice) and Fresnel lens collectors can be applied for low to medium temperature solar thermal technology. To know the performance of these natural rock materials in real applications, it is recommended that further research be conducted under direct solar radiation.

#### 6 ACKNOWLEDGMENT

This research was funded by Universitas Sebelas Maret under funding scheme Kolaborasi Internasional (KI-UNS) with contract/grant number 228/UN27.22/PT.01.03/2023. The grant is gratefully acknowledged by authors.

## 7 REFERENCES

- [1] Y. Bie *et al.*, "Solar medium-low temperature thermal utilization and effect analysis of boundary condition: A tutorial," *Sol. Energy*, vol. 197, pp. 238–253, Feb. 2020, doi: 10.1016/j.solener.2020.01.016.
- [2] S. Olivernesaraj and P. Sethuramalingam, "Atomic Force Microscopy Exploration and Optical Characteristics Analysis of Nanosecond Fiber Laser Micro-textured Single-Crystal Silicon Surfaces," *J. Mater. Eng. Perform.*, Sep. 2022, doi: 10.1007/s11665-022-07293-3.
- [3] H. G. Nguyen *et al.*, "Natural Cellulose Fiber-Derived Photothermal Aerogel for Efficient and Sustainable Solar Desalination," *Langmuir*, vol. 39, no. 19, pp. 6780–6793, May 2023, doi: 10.1021/acs.langmuir.3c00297.
- [4] H. Zhang *et al.*, "Porous Hydrogel Photothermal Conversion Membrane to Facilitate Water Purification," *Langmuir*, vol. 39, no. 21, pp. 7345–7352, May 2023, doi: 10.1021/acs.langmuir.3c00427.
- [5] W. Qiu, S. Xiao, Y. Tong, and S. Yang, "Toward Efficient Charge Collection and Light Absorption: A Perspective of Light Trapping for Advanced Photoelectrodes," *J. Phys. Chem. C*, vol. 123, no. 31, pp. 18753–18770, Aug. 2019, doi: 10.1021/acs.jpcc.9b01533.
- [6] A. F. Mohamed, A. A. Hegazi, G. I. Sultan, and E. M. S. El-Said, "Enhancement of a solar still performance by inclusion the basalt stones as a porous sensible absorber: Experimental study and thermo-economic analysis," *Sol. Energy Mater. Sol. Cells*, vol. 200, p. 109958, Sep. 2019, doi: 10.1016/j.solmat.2019.109958.
- [7] A. Bilal, B. Jamil, N. U. Haque, and M. A. Ansari, "Investigating the effect of pumice stones sensible heat storage on the performance of a solar still," *Groundw. Sustain. Dev.*, vol. 9, p. 100228, Oct. 2019, doi: 10.1016/J.GSD.2019.100228.
- [8] T. Arunkumar, J. Wang, D. Dsilva Winfred Rufuss, D. Denkenberger, and A. E. Kabeel, "Sensible desalting: Investigation of sensible thermal storage materials in solar stills," *J. Energy Storage*, vol. 32, p. 101824, Dec. 2020, doi: 10.1016/j.est.2020.101824.
- [9] L. B. López-Sosa, A. Ortiz-Carrión, D. Espinosa-Gómez, J. Zárate Medina, and M. González-Avilés, "Solar air heating system with low environmental impact materials: Mathematical model and optothermal characterization," *Sustain. Energy Technol. Assessments*, vol. 47, p. 101399, Oct. 2021, doi: 10.1016/j.seta.2021.101399.
- [10] K. Elmaadawy, A. W. Kandeal, A. Khalil, M. R. Elkadeem, B. Liu, and S. W. Sharshir, "Performance improvement of double slope solar still via combinations of low cost materials integrated with glass cooling," *Desalination*, vol. 500, p. 114856, Mar. 2021, doi: 10.1016/j.desal.2020.114856.
- [11] N. Channa Keshava Naik and K. S. Shashi Shekar, "Evaluation and comparison of performance of a solar pebble absorber collector with a conventional flat plate collector," *Mater. Today Proc.*, vol. 52, pp. 266–273, 2022, doi: 10.1016/j.matpr.2021.08.025.
- [12] M. E. H. Attia, A. E. Kabeel, M. E. Zayed, M. Arıcı, and M. Abdelgaied, "Optimal size of spherical rock salt balls as low-cost thermal storage materials for performance augmentation of hemispherical solar distillers: Experimental investigation and thermo-economic analysis," *J. Clean. Prod.*, vol. 374, p. 134006, Nov. 2022, doi: 10.1016/j.jclepro.2022.134006.
- [13] M. Elashmawy, "Improving the performance of a parabolic concentrator solar tracking-tubular solar still (PCST-TSS) using gravel as a sensible heat storage material," *Desalination*, vol. 473, p. 114182, Jan. 2020, doi: 10.1016/J.DESAL.2019.114182.
- [14] J. Sun, Z. Zhang, L. Wang, Z. Zhang, and J. Wei, "Comprehensive Review of Line-Focus Concentrating Solar Thermal Technologies: Parabolic Trough Collector (PTC) vs Linear Fresnel Reflector (LFR)," *J. Therm. Sci.*, vol. 29, no. 5, pp. 1097–1124, Oct. 2020, doi: 10.1007/s11630-020-1365-4.
- [15] A. E. Rungasamy, K. J. Craig, and J. P. Meyer, "A review of linear Fresnel primary optical design methodologies," *Sol. Energy*, vol. 224, pp. 833–854, Aug. 2021, doi: 10.1016/j.solener.2021.06.021.
- [16] K. Pandi, S. Venkatachalapathy, and S. Suresh, "Experimental investigation on low concentration nanofluids with Fresnel lens and evacuated tubes for solar applications," *Int. J. Appl. Ceram. Technol.*, vol. 19, no. 4, pp. 2236–2248, Jul. 2022, doi: 10.1111/ijac.14010.
- [17] A. R. Jensen, I. Sifnaios, G. P. Caringal, S. Furbo, and J. Dragsted, "Thermal performance assessment of the world's first solar thermal Fresnel lens collector field," *Sol. Energy*, Mar. 2022, doi: 10.1016/J.SOLENER.2022.01.067.
- [18] A. Asrori and S. H. Susilo, "The development of Fresnel lens concentrators for solar water heaters: a case study in tropical climates," *EUREKA Phys. Eng.*, no. 3, pp. 3–10, May 2022, doi: 10.21303/2461-4262.2022.002441.
- [19] A. Asrori, S. Suparman, S. Wahyudi, and D. Widhiyanuriyawan, "Investigation of steam generation performance on conical cavity receiver by different geometric concentration ratios for fresnel lens solar concentrator," *Eastern-European J. Enterp. Technol.*, vol. 4, no. 8 (106), pp. 6–14, Aug. 2020, doi: 10.15587/1729-4061.2020.209778.

- [20] A. Asrori, S. Suparman, S. Wahyudi, and D. Widhiyanuriyawan, "An experimental study of solar cooker performance with thermal concentrator system by spot Fresnel lens," *Eastern-European J. Enterp. Technol.*, vol. 5, no. 8 (107), pp. 31–41, Oct. 2020, doi: 10.15587/1729-4061.2020.208638.
- [21] F. L. Rashid, M. A. Al-Obaidi, A. J. Mahdi, and A. Ameen, "Advancements in Fresnel Lens Technology across Diverse Solar Energy Applications: A Comprehensive Review," *Energies*, vol. 17, no. 3, p. 569, Jan. 2024, doi: 10.3390/en17030569.
- [22] J. Hong et al., "Photothermal Chemistry Based on Solar Energy: From Synergistic Effects to Practical Applications," *Adv. Sci.*, vol. 9, no. 3, p. 2103926, Jan. 2022, doi: 10.1002/adv.202103926.
- [23] Z. Bao, N. Bing, H.-R. Yao, Y. Zhang, H. Xie, and W. Yu, "Three-Dimensional Interpenetrating Network Phase-Change Composites with High Photothermal Conversion and Rapid Heat Storage and Release," *ACS Appl. Energy Mater.*, vol. 4, no. 8, pp. 7710–7720, Aug. 2021, doi: 10.1021/acsaem.1c01061.
- [24] W. Zhang, Z. Ling, X. Fang, and Z. Zhang, "Anisotropically conductive Mg(NO<sub>3</sub>)<sub>2</sub>·6H<sub>2</sub>O/g-C<sub>3</sub>N<sub>4</sub>-graphite sheet phase change material for enhanced photo-thermal storage," *Chem. Eng. J.*, vol. 430, p. 132997, Feb. 2022, doi: 10.1016/j.cej.2021.132997.
- [25] Y. Liu et al., "All-Day Anti-Icing/De-Icing Coating by Solar-Thermal and Electric-Thermal Effects," *Adv. Mater. Technol.*, vol. 6, no. 11, p. 2100371, Nov. 2021, doi: 10.1002/admt.202100371.
- [26] W. Wang, F. Ye, J. Dutta, and B. Laumert, "Photothermal performance of three chromia-forming refractory alloys for high-temperature solar absorber applications," *Appl. Therm. Eng.*, vol. 225, p. 120189, May 2023, doi: 10.1016/j.applthermaleng.2023.120189.
- [27] W. Zhu, X. Zuo, Y. Ding, H. Yan, Y. An, and W. Yang, "Experimental investigation on the photothermal conversion performance of cuttlefish ink nanofluids for direct absorption solar collectors," *Appl. Therm. Eng.*, vol. 221, p. 119835, Feb. 2023, doi: 10.1016/j.applthermaleng.2022.119835.
- [28] P. Mu et al., "Conductive hollow kapok fiber-PPy monolithic aerogels with excellent mechanical robustness for efficient solar steam generation," *J. Mater. Chem. A*, vol. 7, no. 16, pp. 9673–9679, 2019, doi: 10.1039/C8TA12243A.
- [29] J. Jia, W. Liang, H. Sun, Z. Zhu, C. Wang, and A. Li, "Fabrication of bilayered attapulgite for solar steam generation with high conversion efficiency," *Chem. Eng. J.*, vol. 361, pp. 999–1006, Apr. 2019, doi: 10.1016/j.cej.2018.12.157.
- [30] H. W. Lim, S. H. Park, and S. J. Lee, "3D thermoresponsive hydrogel with enhanced water uptake and active evaporation for effective interfacial solar steam generation," *Desalination*, vol. 550, p. 116368, Mar. 2023, doi: 10.1016/j.desal.2022.116368.
- [31] C.-Y. Zhao et al., "Falling film evaporation in a triangular tube bundle under the influence of cross vapor stream," *Int. J. Refrig.*, vol. 112, pp. 44–55, Apr. 2020, doi: 10.1016/j.ijrefrig.2019.12.028.
- [32] A. Rajiv Krishnan and K. D., "Influence of heat absorber materials sand, soil and paraffin wax in solar still on sustainable water distillation," *Case Stud. Chem. Environ. Eng.*, vol. 8, p. 100365, Dec. 2023, doi: 10.1016/j.cscee.2023.100365.
- [33] E. H. Alaskaree, "An experimental investigation of the solar distiller basin's performance using a flat mirror and vertical barriers," *Case Stud. Chem. Environ. Eng.*, vol. 8, p. 100416, Dec. 2023, doi: 10.1016/j.cscee.2023.100416.
- [34] V. Sousa and I. Meireles, "Dynamic simulation of the energy consumption and carbon emissions for domestic hot water production in a touristic region," *J. Clean. Prod.*, vol. 355, p. 131828, Jun. 2022, doi: 10.1016/j.jclepro.2022.131828.
- [35] M. Z. Pomianowski, H. Johra, A. Marszal-Pomianowska, and C. Zhang, "Sustainable and energy-efficient domestic hot water systems: A review," *Renew. Sustain. Energy Rev.*, vol. 128, p. 109900, Aug. 2020, doi: 10.1016/j.rser.2020.109900.
- [36] M. Wirawan, M. Mirmanto, and I. Fahrurrozi, "The Influence of the Tilt Angle of a Flat Plate Solar Collector with Granite Stone Absorber on Its Performance," *Int. J. Adv. Eng. Manag.*, vol. 5, no. 4, pp. 1234-1238 w, 2023, doi: 10.35629/5252-050412341238.
- [37] R. Kumar et al., "Experimental investigation of impact of the energy storage medium on the thermal performance of double pass solar air heater," *Sustain. Energy Technol. Assessments*, vol. 48, p. 101673, Dec. 2021, doi: 10.1016/j.seta.2021.101673.
- [38] C. Zing, S. Mahjoob, and K. Vafai, "Analysis of porous filled heat exchangers for electronic cooling," *Int. J. Heat Mass Transf.*, vol. 133, pp. 268–276, Apr. 2019, doi: 10.1016/j.ijheatmasstransfer.2018.12.067.
- [39] X. Zhai, H. Ge, T. Wang, C.-M. Shu, and J. Li, "Effect of water immersion on active functional groups and characteristic temperatures of bituminous coal," *Energy*, vol. 205, p. 118076, Aug. 2020, doi: 10.1016/j.energy.2020.118076.
- [40] A. Midilli, "Determination of pistachio drying behaviour and conditions in a solar drying system," *Int. J. Energy Res.*, vol. 25, no. 8, pp. 715–725, Jun. 2001, doi: 10.1002/er.715.

- [41] M. Vinod, M. Raghuraman, and V. M. Chakravarthi, "Experimental Investigation of Paddy Grain Drying Mechanism," 2020, pp. 135–143.
- [42] E. Duque-Dussán, J. R. Sanz-Urbe, and J. Banout, "Design and evaluation of a hybrid solar dryer for postharvesting processing of parchment coffee," *Renew. Energy*, vol. 215, p. 118961, Oct. 2023, doi: 10.1016/j.renene.2023.118961.
- [43] F. Kulapichitr, C. Borompichaichartkul, I. Suppavorasatit, and K. R. Cadwallader, "Impact of drying process on chemical composition and key aroma components of Arabica coffee," *Food Chem.*, vol. 291, pp. 49–58, Sep. 2019, doi: 10.1016/j.foodchem.2019.03.152.
- [44] A. Lingayat, R. Balijepalli, and V. P. Chandramohan, "Applications of solar energy based drying technologies in various industries – A review," *Sol. Energy*, vol. 229, pp. 52–68, Nov. 2021, doi: 10.1016/j.solener.2021.05.058.
- [45] S. H. Farjana, N. Huda, and M. A. P. Mahmud, "Industry-Specific Utilization of Solar Industrial Process Heat (SHIP)," in *Nanostructured Materials for Next-Generation Energy Storage and Conversion*, Berlin, Heidelberg: Springer Berlin Heidelberg, 2019, pp. 409–438.
- [46] L. Wang, Y. Feng, K. Wang, and G. Liu, "Solar water sterilization enabled by photothermal nanomaterials," *Nano Energy*, vol. 87, p. 106158, Sep. 2021, doi: 10.1016/j.nanoen.2021.106158.
- [47] A. S. Isah, S. H. Bt Shafiai, H. B. Takaijudin, B. Singh Mahinder Singh, and S. I. U. H. Gilani, "The role of desalination and contribution of hybrid solar desalination system towards primary health care," *Case Stud. Chem. Environ. Eng.*, vol. 6, p. 100253, Dec. 2022, doi: 10.1016/j.cscee.2022.100253.
- [48] P. Udomkun et al., "Review of solar dryers for agricultural products in Asia and Africa: An innovation landscape approach," *J. Environ. Manage.*, vol. 268, p. 110730, Aug. 2020, doi: 10.1016/j.jenvman.2020.110730.
- [49] H. Liu, J. Y. Lim, B. Wint Hnin Thet, P.-Y. Lai, and W. S. Koh, "Evaluating the impact of tree morphologies and planting densities on outdoor thermal comfort in tropical residential precincts in Singapore," *Build. Environ.*, vol. 221, p. 109268, Aug. 2022, doi: 10.1016/j.buildenv.2022.109268.
- [50] W. W. Burchett, A. R. Ellis, S. W. Harrar, and A. C. Bathke, "Nonparametric Inference for Multivariate Data: The R Package nrmv," *J. Stat. Softw.*, vol. 76, no. 4, 2017, doi: 10.18637/jss.v076.i04.
- [51] S. Ma, W. Qarony, M. I. Hossain, C. T. Yip, and Y. H. Tsang, "Metal-organic framework derived porous carbon of light trapping structures for efficient solar steam generation," *Sol. Energy Mater. Sol. Cells*, vol. 196, pp. 36–42, Jul. 2019, doi: 10.1016/j.solmat.2019.02.035.
- [52] Y. Li et al., "Manipulating light trapping and water vaporization enthalpy via porous hybrid nanohydrogels for enhanced solar-driven interfacial water evaporation with antibacterial ability," *J. Mater. Chem. A*, vol. 7, no. 47, pp. 26769–26775, 2019, doi: 10.1039/C9TA09820H.
- [53] R. Gao et al., "Light trapping induced flexible wrinkled nanocone SERS substrate for highly sensitive explosive detection," *Sensors Actuators B Chem.*, vol. 314, p. 128081, Jul. 2020, doi: 10.1016/j.snb.2020.128081.
- [54] X. Yu et al., "Enhancement of photo-thermal performance using hole plasmonic nanofluids," *Appl. Therm. Eng.*, vol. 236, p. 121868, Jan. 2024, doi: 10.1016/j.applthermaleng.2023.121868.
- [55] A. Chen et al., "Magnetic-directed fillers migration during micro-injection molding of magnetic polypropylene nanocomposite surfaces with uplifted light trapping microarchitectures for freezing delay and photothermal-enhanced de-icing," *Appl. Therm. Eng.*, vol. 230, p. 120810, Jul. 2023, doi: 10.1016/j.applthermaleng.2023.120810.
- [56] Q. Huang, C. Du, and C. Huang, "Nature-inspired pyramid-shaped 3-dimensional structure for cost-effective heat-localized solar evaporation with high efficiency and salt localization," *Appl. Therm. Eng.*, vol. 215, p. 118950, Oct. 2022, doi: 10.1016/j.applthermaleng.2022.118950.
- [57] W. He, L. Zhou, M. Wang, Y. Cao, X. Chen, and X. Hou, "Structure development of carbon-based solar-driven water evaporation systems," *Sci. Bull.*, vol. 66, no. 14, pp. 1472–1483, Jul. 2021, doi: 10.1016/j.scib.2021.02.014.
- [58] X.-H. Gao, Z.-M. Guo, Q.-F. Geng, P.-J. Ma, and G. Liu, "Microstructure and Optical Properties of SS/Mo/Al<sub>2</sub>O<sub>3</sub> Spectrally Selective Solar Absorber Coating," *J. Mater. Eng. Perform.*, vol. 26, no. 1, pp. 161–167, Jan. 2017, doi: 10.1007/s11665-016-2445-1.
- [59] M. Amjad, H. Jin, X. Du, and D. Wen, "Experimental photothermal performance of nanofluids under concentrated solar flux," *Sol. Energy Mater. Sol. Cells*, vol. 182, pp. 255–262, Aug. 2018, doi: 10.1016/j.solmat.2018.03.044.
- [60] P. Kalidoss, S. G. Venkatachalapathy, and S. Suresh, "Photothermal performance of hybrid nanofluids with different base fluids for solar energy applications," *Energy Sources, Part A Recover. Util. Environ. Eff.*, pp. 1–16, Jun. 2021, doi: 10.1080/15567036.2021.1936697.
- [61] M. Mehrali, M. K. Ghatkesar, and R. Pecnik, "Full-spectrum volumetric solar thermal conversion via graphene/silver hybrid plasmonic nanofluids," *Appl. Energy*, vol. 224, pp. 103–115, Aug. 2018, doi: 10.1016/j.apenergy.2018.04.065.

- [62] Z. Li, A. Kan, K. Wang, Y. He, N. Zheng, and W. Yu, "Optical properties and photothermal conversion performances of graphene based nanofluids," *Appl. Therm. Eng.*, vol. 203, p. 117948, Feb. 2022, doi: 10.1016/j.applthermaleng.2021.117948.
- [63] J. Qu, L. Shang, Q. Sun, X. Han, and G. Zhou, "Photo-thermal characteristics of water-based graphene oxide (GO) nanofluids at reverse-irradiation conditions with different irradiation angles for high-efficiency solar thermal energy harvesting," *Renew. Energy*, vol. 195, pp. 516–527, Aug. 2022, doi: 10.1016/j.renene.2022.06.049.
- [64] X. Zuo *et al.*, "Silicon dioxide coating nanocomposites and cellulose-modified stable nanofluid for direct absorption solar collection," *Sol. Energy*, vol. 262, p. 111797, Sep. 2023, doi: 10.1016/j.solener.2023.111797.
- [65] J. Wen, X. Li, W. Chen, and J. Liu, "Systematical investigation on the solar-thermal conversion performance of TiN plasmonic nanofluids for the direct absorption solar collectors," *Colloids Surfaces A Physicochem. Eng. Asp.*, vol. 624, p. 126837, Sep. 2021, doi: 10.1016/j.colsurfa.2021.126837.
- [66] E. Abed, R.N; Abded, A.R.N; Yousif, "Carbon Surfaces Doped with (Co<sub>3</sub>O<sub>4</sub>-Cr<sub>2</sub>O<sub>3</sub>) Nanocomposite for High-Temperature Photo Thermal Solar Energy Conversion Via Spectrally Selective Surfaces," *Prog. Color. Color. Coatings J.*, vol. 14, no. 1, pp. 301–3015, 2021, doi: 10.30509/PCCC.2021.166749.1098.
- [67] K. Han, Y. Wang, S. Wang, Q. Liu, Z. Deng, and F. Wang, "Narrowing band gap energy of CeO<sub>2</sub> in (Ni/CeO<sub>2</sub>)@SiO<sub>2</sub> catalyst for photothermal methane dry reforming," *Chem. Eng. J.*, vol. 421, p. 129989, Oct. 2021, doi: 10.1016/j.cej.2021.129989.

Paper submitted: 22.11.2023.

Paper accepted: 04.03.2024.

This is an open access article distributed under the CC BY 4.0 terms and conditions